Int. J. Heat Mass Transfer. Vol. 25, No. 7, pp. 1013–1022, 1982
Printed in Great Britain

0017–9310/82/071013–10 $03.00/0
Pergamon Press Ltd.

STUDIES ON THERMOHYDRAULICS OF SINGLE- AND MULTI-START SPIRALLY CORRUGATED TUBES FOR WATER AND TIME-INDEPENDENT POWER LAW FLUIDS

S. GANESHAN and M. RAJA RAO
Department of Chemical Engineering, Institute of Technology, Bombay 400 076, India

(*Received* 22 *May* 1981 *and in final form* 10 *November* 1981)

Abstract—Results are presented from an experimental investigation of the tube side friction and heat transfer behaviour of one smooth tube and seven spirally corrugated tubes of one to four helical starts, having the same helix angle 65° for a wide range of the geometrical aspect ratios (h/D_i), (p/h) and (p/D_i) characterizing the surface roughness. Based on the analogy between heat and momentum transfer, friction and heat transfer correlations are developed to fit the experimental data. On the criterion of heat exchanger capacity per unit pumping power, the four-start corrugated tubes are found to be 100% more efficient than a smooth tube for heating of water ($Pr = 4.3$) and 150% more efficient for heating of the more viscous liquids of high Prandtl number ($Pr_d = 109$).

NOMENCLATURE

A_i, tube inside area [m^2];
C_p, specific heat [$kJ\,kg^{-1}\,K^{-1}$];
D, D_i, tube inside diameter [m];
h, roughness height [m];
h_i, tube inside heat transfer coefficient [$W\,m^{-2}\,K^{-1}$];
k, thermal conductivity [$W\,m^{-1}\,K^{-1}$];
K', flow consistency index [$Ns^{n'}\,m^{-2}$];
L, length [m];
n', flow behaviour index;
N, number of groove starts;
p, pitch of corrugation [m];
p', effective pitch [$p\,N^{-1}$];
ΔP, pressure drop [$N\,m^{-2}$];
Q, heat transfer rate [W];
R, radius of tube [m];
T, temperature [°C];
u^*, shear velocity [$m\,s^{-1}$];
V, bulk average velocity [$m\,s^{-1}$];
w, width of corrugation [m];
y, radial distance from the wall [m].

Greek symbols

μ, dynamic viscosity [$Ns\,m^{-2}$];
μ_d, differential viscosity [$Ns\,m^{-2}$];
ν, kinematic viscosity [$m^2\,s^{-1}$];
ρ, density [$kg\,m^{-3}$];
τ, shear stress [$N\,m^{-2}$];
α, helix angle [degrees].

Dimensionless groups

f, friction factor, $2\tau_w(g/c)/\rho V^2$;
$G(h^+, Pr)$ heat transfer roughness function $R(h^+) + (f/2St - 1)/\sqrt{(f/2)}$;
h^+, roughness Reynolds number $hu^*/\nu = Re\sqrt{(f/2)}(h/D)$;
Nu, Nusselt number, (hD/k);
Pr, Prandtl number, $(C_p\mu/k)$;
Pr_d, generalised Prandtl number, $= (C_pK'/k)(8V/D)^{(n'-1)}[4n'^2/(3n' + 1)]$;
Re, Reynolds number, $(DV\rho/\mu)$;
Re_d, generalised Reynolds number, $= (D^{n'}V^{2-n'}\rho/K'8^{n'-1})(3n' + 1/4n'^2)$;
$R(h^+)$, momentum transfer roughness function, $(\sqrt{2/f}) + 2.5\ln(2h/D) + 3.75$;
St, Stanton number, $h/(V\rho C_p)$;
u^+, dimensionless velocity, u/u^*;
y^+, dimensionless radial distance from the wall, yu^*/ν;
t^+, dimensionless temperature, $(T_w - T)(C_p\rho u^*)/q$.

Subscripts

a, augmented tube;
b, bulk condition;
i, based on inside diameter;
m, mean value, at radial distance from the wall where $u = u_m$;
0, equivalent smooth tube value;
t, turbulent flow condition;
w, wall condition.

INTRODUCTION

THE NEED to conserve energy and materials has stimulated the search for various methods of augmenting heat transfer and some of the modern techniques include the use of convergent–divergent type and plate type heat exchangers. Further, various turbulation techniques are used to improve the tube side heat transfer coefficients for convective heat transfer and many of these involve the penalty of increased pressure drop and pumping power. Internal roughness such as

sand-grain textures [1–3] transverse ribbing, [4–8] internal fins [9, 10] and wire coils [11] have been studied or applied with varying degrees of success. The spirally corrugated tubes investigated for a few heat exchange applications [12–17] provide several advantages over other rough surfaces such as (i) the increase in pressure drop is often more than compensated by the increase in the heat transfer coefficient (ii) no material is added to or removed from the tube (iii) the fabrication is easier. However, no systematic study of these tubes with single start and multi-start configurations has been made with a view to develop correlations based on heat and momentum transfer analogies and also to make a parametric evaluation of the tubes for different heat exchanger applications.

ROUGH SURFACE ANALYSIS

The flow over a rough surface is not sufficiently understood to permit heat transfer and friction prediction by analytical methods, and law of the wall similarity is, however, a reasonably well accepted concept. The law of the wall and velocity defect law, applicable respectively for the inner and outer regions of the turbulent boundary layer, are combined to give the following velocity distribution equations for the turbulence-dominated regions of the wall region, the constants being proposed by Nikuradse [18] on the basis of measured velocity distributions:

$$u^+ = 2.5 \ln y^+ + 5.5 \text{ (smooth tube)}, \quad (1)$$

$$u^+ = 2.5 \ln(y/h) + R(h^+) \text{ (rough tube)}. \quad (2)$$

Equation (2) gives on integration

$$R(h^+) = \sqrt{(2/f)} + 2.5 \ln (2h/D_i) + 3.75. \quad (3)$$

Nikuradse [18] correlated his pressure drop results for tubes having sand-grain roughness by plotting $R(h^+)$ as a function of the roughness Reynolds number (h^+) given by

$$h^+ = hu^*/\nu = (h/D_i)Re\sqrt{(f/2)} \quad (4)$$

For the fully rough region ($h^+ > 70$), Nikuradse obtained a constant value of 8.48 for $R(h^+)$. For the hydraulically smooth region ($h^+ \leq 5$), $R(h^+)$ is given by

$$R(h^+) = 2.5 \ln h^+ + 5.5. \quad (5)$$

This equation (5) combined with equation (2) gives the equation (1) for u^+ for a smooth tube for turbulent core ($y^+ > 30$).

Webb *et al.* [5] used the same correlation method for their friction data for geometrically similar repeated rib roughness, and found that different values of $R(h^+)$ are obtained for the repeated-rib and sand-grain roughness. The authors found that $R(h^+)$ is a function of (p/h) and correlated their results by using the equation

$$R(h^+) = 0.95(p/h)^{0.53} \quad (\text{for } h^+ > 35). \quad (6)$$

Assuming that the law of wall similarity applies to the temperature profile as well as to the velocity profile, Dipprey and Sabersky [2] developed a heat-momentum transfer analogy relationship for flow in a sand-grain roughened tube, given by

$$(f/2St - 1)/(\sqrt{f/2}) + R(h^+) = G(h^+, Pr) \quad (7)$$

and correlated their results for the fully rough region ($h^+ > 70$) by the equation

$$(f/2St - 1)/(\sqrt{f/2}) + 8.48 = 5.19\, Pr^{0.44} (h^+)^{0.20}. \quad (8)$$

Webb *et al.* [5] correlated their heat transfer results for tubes with repeated rib roughness, not considering the small effect of (p/h) in their correlation

$$(f/2St - 1)/\sqrt{(f/2)} + R(h^+) = 4.75(Pr)^{0.57} (h^+)^{0.28} \quad (\text{for } h^+ > 25) \quad (9)$$

Dodge and Metzner [19] extended the friction similarity law to non-Newtonian (power law) fluids and obtained a velocity profile equation, which for Newtonian fluids, reduces to the equation (1) of Nikuradse for smooth tubes. Thus $R(h^+)$ for power law fluids would be a function of flow behaviour index, n' besides the geometrical parameters defining surface roughness. Since no previous work was reported on evaluating and correlating $R(h^+)$ and $G(h^+)$ functions for non-Newtonian power law fluids, the present investigation was undertaken with the object of studying the thermohydraulics of spirally corrugated tubes with single-start and multi-start helical groove configurations for power law fluids and proposing design correlations based on heat and momentum transfer analogies, and making parametric evaluation of the tubes for a particular heat exchanger application.

EXPERIMENTAL

Tube configuration

In the present investigation seven spirally corrugated tubes and one smooth tube, (25 mm I.D. and 28 mm O.D.) all of copper material were used. Their dimensions are presented in Table 1. Smooth tube was used for standardizing the experimental set up and also to compare the enhancement obtained in heat transfer and friction factor. Tubes 1–4 were fabricated from plain copper tubes by single-spiral indenting, which embosses an internal projection (ridge), in registration with an external helical groove. This configuration was attainable without thinning the tube wall at the focus of the corrugation. Tubes 5–7 were fabricated to have two-, three- and four helical starts, but all having the same helical angle ($\alpha = 65°$) as tubes 1–4. In the case of multi-start tubes, pitch is defined as the axial distance through which one ridge or crest makes a 360° turn along the tube circumference. The effective pitch (p') is thus the pitch divided by the number of helical starts. The dimensionless aspect ratios (p/h), (h/D) and (p/D) are useful in correlating the frictional and heat transfer characteristics of the corrugated tubes.

Table 1. Characteristic dimensions of the spirally corrugated tubes

S. No.	Tube No.	D_0 (mm)	D_i (mm)	h (mm)	w (mm)	p (mm)	N	p'	h/D_i	p'/h	p'/D_i	α
1	S	28.0	25.0						0	∞	∞	
2	1	28.66	25.66	0.67	2.81	30.0	1	30	0.0261	44.78	1.169	65
3	2	28.44	25.44	0.53	3.30	30.0	1	30	0.0208	56.60	1.179	65
4	3	28.70	25.70	0.63	4.05	30.0	1	30	0.0245	47.62	1.167	65
5	4	28.38	25.38	0.77	5.85	30.0	1	30	0.0303	38.96	1.182	65
6	5	28.22	25.22	0.35	2.46	30.0	2	15	0.0139	42.86	0.595	65
7	6	28.45	25.45	0.30	2.43	30.0	3	10	0.0118	33.33	0.393	65
8	7	28.26	25.26	0.59	2.73	30.0	4	7.5	0.0233	12.71	0.297	65

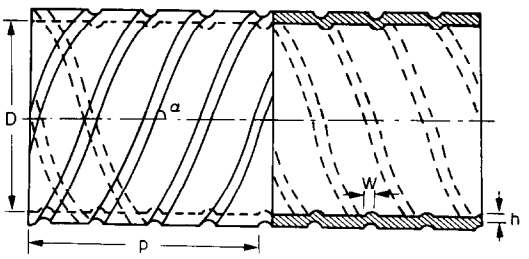

FIG. 1. Characteristic parameters of a spirally corrugated tube. h, height of corrugation, w, width of corrugation, p, pitch of corrugation, D, diameter of tube, α, helix angle.

A section of the four-start corrugated tubes used is shown in Fig. 1. All the tubes were manufactured by Spirance Corporation, Bombay.

Test liquids

The test liquids used were water, 0.30, 0.50 and 0.75% SCMC solutions. The rheological properties of the polymer solutions were determined by a capillary tube viscometer and are listed in Table 2. These solutions were found to be pseudoplastic in nature and obeyed the generalised power law model [20]

$$\tau_w = D\Delta P/4L = K'(8V/D)^{n'}. \quad (10)$$

For these dilute aqueous polymer solutions, ρ, C_p and K' were found to be the same as those of water within 1–2%.

Apparatus

A schematic diagram of the experimental set up is shown in Fig. 2. The actual test section consisted of a 3000 mm long double pipe heat exchanger, the inner tube of which was either the smooth tube or a spirally corrugated tube under test. The outer tube was a 50 mm I.D. galvanised iron pipe, having openings, at every 250 mm distance, radially displaced by 180°, for the passage of copper–constantan thermocouple leads. Thirteen such thermocouples were embedded in the exchanger tube wall for the measurement of wall temperature. The test section was preceded and followed by smooth tube or spirally corrugated tube calming sections, each 1250 mm long, depending on the tube under test.

The isothermal pressure drop studies were conducted at 30°C in all the tubes for turbulent flow of water and the three aqueous polymer solutions and steady state pressure drop was measured by means of U-tube manometers using mercury or carbon tetrachloride as manometric liquids. Steady state flow rate of the test liquid was obtained from a precision calibrated rotameter.

Heat transfer studies were carried out in turbulent flow inside the inner tube of the heat exchanger using hot water (as heating medium) flowing at a constant temperature in the annulus of the exchanger. Steady state flow rates of hot water and test liquid were obtained from calibrated rotameters. The incoming

Table 2. Rheological properties of the pseudoplastic solutions

Solution	Temperature (°C)	n'	$K' \times 10^2$ ($NS^{n'} m^{-2}$)
0.30% SCMC	30	0.93	0.583
	40	0.93	0.492
	50	0.93	0.382
	60	0.93	0.324
0.50% SCMC	30	0.85	3.24
	40	0.85	2.70
	50	0.85	2.19
	60	0.85	1.74
0.75% SCMC	30	0.82	8.14
	40	0.82	6.76
	50	0.82	5.21
	60	0.82	4.23

and outgoing temperatures of exchanger fluids were measured by calibrated precision thermometers, and the metal wall temperature obtained from a precision temperature recorder.

RESULTS AND DISCUSSION

Friction factor

The Fanning's friction factor was calculated from the equation

$$f = D\Delta P/2\rho LV^2. \tag{11}$$

The smooth tube turbulent flow friction factors for water were well correlated by the Blasius equation

$$f = 0.079(Re)^{-0.25} \tag{12}$$

for $4000 < Re < 1.5 \times 10^5$ with a standard deviation of 2.5% and this served the purpose of standardization of the flow setup. Further, the smooth tube turbulent friction factors agreed within 10% of those calculated by the Dodge–Metzner [19] equation for the three pseudoplastic polymer solutions

$$1/f^{1/2} = 4.0/n'^{0.75} \log [Re_{gen}(f)^{(1-n'/2)}] - 0.40/n'^{1.2} \tag{13}$$

where

$$Re_{gen} = \frac{D^{n'} V^{2-n'} \rho}{K' 8^{(n'-1)}}. \tag{14}$$

Further, Re_d based on μ_d was defined as

$$Re_d = \frac{D^{n'} V^{2-n'} \rho}{K' 8^{n'-1}} \frac{(3n'+1)}{(4n'^2)} = Re_{gen} \frac{(3n'+1)}{(4n'^2)}. \tag{15}$$

At a constant Reynolds number, the friction factors

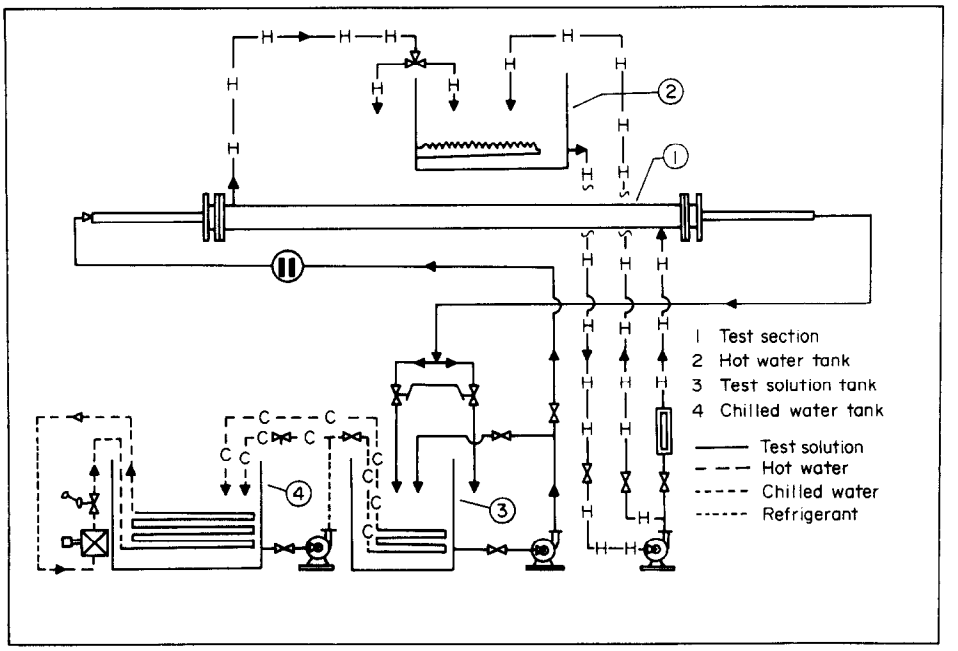

FIG. 2. Schematic diagram of the experimental set-up.

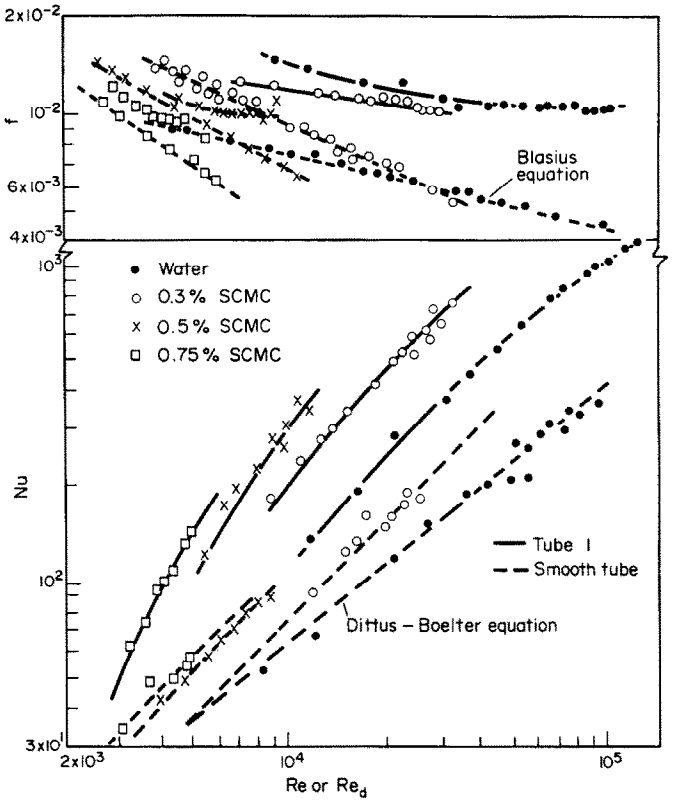

FIG. 3. Variation of f and Nu with Re.

of all the test liquids were found to be higher in spirally corrugated tubes than in a smooth tube, and this is clear from an inspection of Fig. 3, showing results for a typical corrugated tube 1.

The friction factor for tube 1 was improved by a factor of 2–2.3 for water (for $10^4 < Re < 10^5$), compared to 1.2–1.6 only for the more viscous 0.75% SCMC (for $3000 < Re_d < 7000$). On the other hand, the rougher tube 7 with four helical starts ($p' = 7.5$ cm) gave still greater friction enhancement of 3.0–3.5 times for water, and 1.7–2.0 times for 0.75% SCMC.

The tubes 5 and 6 having two and three starts but with a lower corrugation height of 0.30–0.35 mm were noted to give slightly lower values of friction factor enhancement compared to tube 1 at any Reynolds number of a test liquid.

A characteristic feature of flow in a spirally corrugated tube is that friction factor continues to decrease with Reynolds number even at higher flow rates—a behaviour earlier reported by Gupta and Rao [15], as due to the spiral flow superimposed on the main axial flow. Further, the dependence of f on Re was found to decrease with markedly severe surface roughness, resulting from larger height (h) and smaller (effective) pitch (p') of corrugation.

Heat transfer

The inside heat transfer coefficient of the test liquid was calculated by the equation

$$Q = h_i A_i (T_w - T_b)_{l.m}. \quad (16)$$

The inside coefficient h_i was expressed as Nusselt number, $(h_i D_i/K)$ which was plotted against Re (or Re_d) in Fig. 3 for the smooth tube and a typical spirally corrugated tube 1 for the four test liquids used ($4.3 < Pr < 109$). Experimental turbulent flow Nusselt numbers for water in the smooth tube agreed closely within 3% of the values predicted by Dittus–Boelter equation

$$Nu = h_i D_i/K = 0.023\, Re^{0.8}\, Pr^{0.4}. \quad (17)$$

The experimental turbulent Nusselt numbers of the aqueous polymer solutions in the smooth tube were correlated by the following equation

$$Nu = 0.00160\, Re_{gen}^{1.045}\, Pr_{gen}^{0.40} = 0.0014\, Re_d^{1.045}\, Pr_d^{0.40} \quad (18)$$

where [20]

$$Pr_{gen} = (C_p K'/k)/K' (8V/D)^{n'-1};$$

$$Pr_d = (C_p K'/k)/K' (8V/D)^{n'-1} [4n'^2/(3n' + 1)]. \quad (19)$$

The exponent 1.045 of generalised Reynolds number agreed closely with the value of 0.99, obtained by Clapp [21] for power law fluids.

At a constant Reynolds number, the Nusselt numbers for the turbulent heating of test liquids in spirally corrugated tubes are higher by a factor of 1.8–3.0,

depending upon the tube wall roughness and Prandtl number of the test liquid. The functional relationship of Nusselt number with the Reynolds number might not be the same for smooth and rough tubes, in view of the fact that both Kidd [13] and Gupta and Rao [15] have noted the exponent of Re in Nu–Re relationship to be greater than 0.8, and which is a unique function of surface roughness, especially for very rough tubes. Watkinson *et al.* [9] have however reported a Reynolds number exponent of 0.6, for water heating in tubes with internal integral spiral fins. This fact underlines the importance of determining the tube side heat transfer coefficients directly, without resorting to the Wilson plot technique which was used by Withers *et al.* [14]. As this technique assumes the exponent of Re as 0.8, it might give inaccurate h_i values for rough tubes.

Friction correlation

The results of friction factor in spirally corrugated tubes are analysed in terms of momentum transfer roughness function $R(h^+)$, which is plotted as a function of (h^+) in Fig. 4 for all the seven tubes for water as well as 0.75% SCMC. Although tubes 1–4 are essentially geometrically similar (p/h = 39–56), their groove width varies from 2.81 to 5.85 mm, due to which the data are vertically displaced for these tubes 6 and 2, and are the lowest for the rougher tube 7. For all the tubes $R(h^+)$ shows a rising trend with increase in h^+, which is similar to the same reported recently by Withers [17] for single-helix corrugated tubes for turbulent flow of water.

Unlike for repeated rib roughness, $R(h^+)$ for corrugated tubes was not independent of h^+ in the fully rough region (for $h^+ > 70$), and it increased with increasing h^+, due to the unique nature of flow in these tubes, wherein f is a function of Re even in highly turbulent flow conditions. In general, the greater is the Prandtl number of test liquid, the flow will be more in the transition region ($3 < h^+ < 70$). With water, however, it is possible to cover transition and fully rough regions, since h^+ values ranged from around 10–300.

In the present study, h^+ values less than 10 could be obtained only for the more viscous pseudoplastic test solutions. Dodge and Metzner [19] have shown that the laminar sub-layer for pseudoplastic fluids would be thinner than for Newtonian fluids. Thus the spirally corrugated tubes continue to behave as rough surfaces, even at lower h^+ values, for pseudoplastic fluids.

Dalle Donne and Meyer [7] found that inter-rib spacing $(p - w)$ is a more significant parameter than pitch (p) in view of the lack of influence of rib width (w) on the transfer process, which is controlled by the repeated separation and reattachment of flow. Thus, by cross-plotting, $R(h^+)$ was found to vary with $[h/(p-w)]^{-0.52}$. Webb *et al.* [5] also found that for $h^+ > 26$ $R(h^+)$ correlated well with $(h/p)^{-0.53}$. The effect of increased number of groove starts (N) was to increase f, and $R(h^+)$ was found to be proportional to $N^{-0.24}$. Further $R(h^+)$ was observed to vary with $n'^{2.5}$. The following correlation fitted the data points in Fig. 5 within a standard deviation of 10%:

$$R(h^+)[h/(p-w)]^{0.52}(N)^{0.24}(n')^{2.5} = 0.273\ln(h^+) + 0.127$$

or

$$h^+ = 0.629\exp[3.66\,R(h^+) + [h/(p-w)]^{0.52}N^{0.24}(n')^{2.5}]. \quad (20)$$

Heat transfer correlation

Values of heat transfer roughness function $G(h^+, Pr)$ were calculated from equation (7), using $R(h^+)$ value for the same value of (h^+) for the given tube and test liquid combination. Variation of $G(h^+, Pr)$ is shown in Fig. 6 as a function of roughness Reynolds number (h^+) for water and 0.75% SCMC.

It is evident that water data cover transition and fully rough regions (h^+ = 10–300), while data for 0.75% SCMC cover part of transition region only (h^+ = 3–20). The data for 0.30% and 0.50% SCMC (not shown) cover partly transition and partly fully rough regions. No significant dependence of $G(h^+, Pr)$ on (p/h) was observed in the present work.

Dalle Donne and Meyer [7] and Webb *et al.* [5] observed that $G(h^+, Pr)$ is essentially independent of rib geometry for internal rib-roughened tubes. Withers [17], however, incorporated the small effect of (p/D_i), by using $G(h^+)(p/D)^{1/3}$ in correlating heat transfer

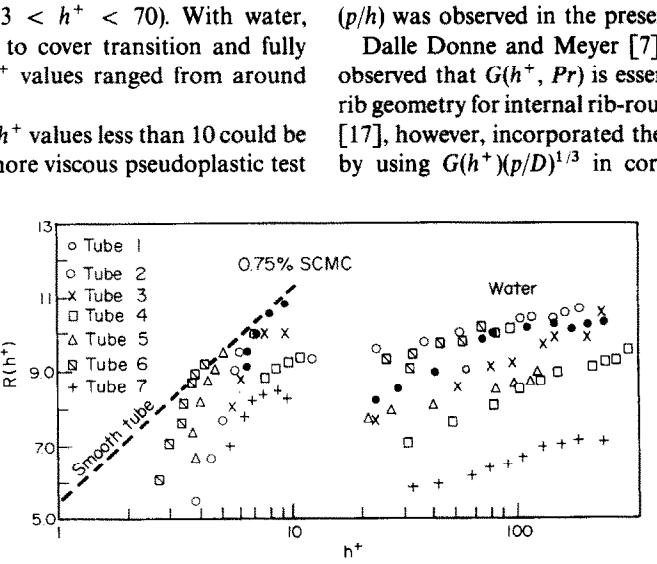

FIG. 4. Variation of $R(h^+)$ with (h^+).

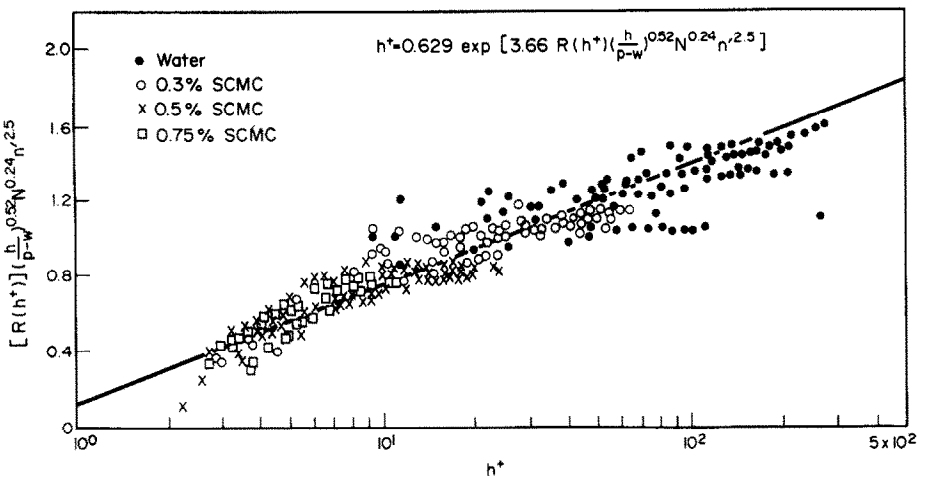

FIG. 5. Variation of $[R(h^+)]\,[h/(p-w)]^{0.52}\,N^{0.24}\,n'^{2.5}$ with roughness Reynolds number (h^+) for the flow of water and aqueous SCMC solutions in spirally corrugated tubes—final correlation.

results for corrugated tubes with internal single-helical ridging. Even then, the heat transfer results for tubes having $(p/D_i) = 0.911$ were 25% higher than those for tubes having $(p/D_i) = 0.337$. Gee and Webb [8] reported that the G-function was influenced by the helix angle of the corrugation. In view of the constant helical angle ($\alpha = 65°$) used with single-start and multi-start tubes of the present study, and the very small effect of (p/D_i) on the heat transfer correlation, (p/D_i) was not included as an argument of the G-function in the heat transfer correlation.

The influence of Prandtl number on the G-function was evaluated by the treatment of the heat transfer results for the four test liquids ($4.3 < Pr < 109$) and $G(h^+, Pr)$ was found proportional to $Pr^{0.55}$. This compared well with the function $Pr^{0.57}$ obtained by Webb *et al.* [5] for repeated-rib roughened tubes. Dipprey and Sabersky [2], however, obtained the function as $Pr^{0.44}$ for sand-grain roughness. The heat transfer results of the present work with multi-start spirally corrugated tubes cover a wider range of roughness Reynolds number ($3 < h^+ < 300$) and Prandtl number ($4.3 < Pr < 109$), and were correlated on the plot of $G(h^+, Pr)Pr^{-0.55}$ against (h^+) in Fig. 7. The solid curve closely represents the data points and the final correlation between $G[(h^+), Pr]\,Pr^{-0.55}$ and (h^+) was obtained as a polynomial function, given by

$$\log [G(h^+, Pr)Pr^{-0.55}] = 2.576 - 1.707 \log h^+ + 0.497 (\log h^+)^2 - 0.0103 (\log h^+)^3. \quad (21)$$

The above equation predicts the value of G-function within a standard deviation of 20%.

The curve in Fig. 7 has a minimum value of $G(h^+, Pr)Pr^{-0.55}$ at $h^+ = 40$, at which the roughness element extends into the turbulent core. For a roughness element to be effective, it should extend well beyond the buffer layer. Webb *et al.* [5] found the minimum at $h^+ = 26$ for rib-type roughness. The wall heat transfer resistance has a minimum value at this minimum point.

The equations of Dipprey and Sabersky [2] for sand-grain roughness and Webb *et al.* [5] for repeated-rib type roughness are also shown as dotted lines in

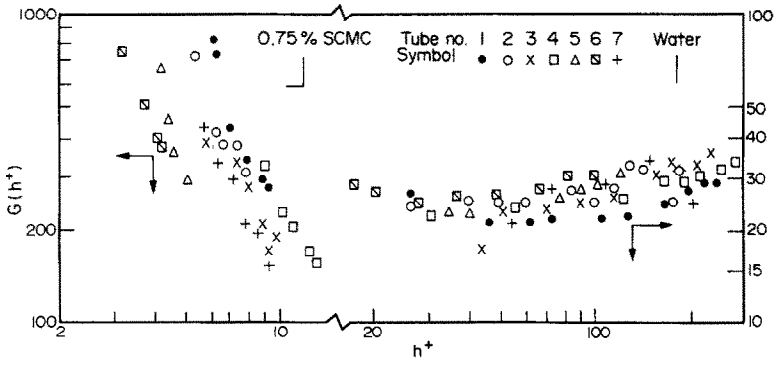

FIG. 6. Variation of $G(h^+)$ with (h^+) for water and 0.75% SCMC.

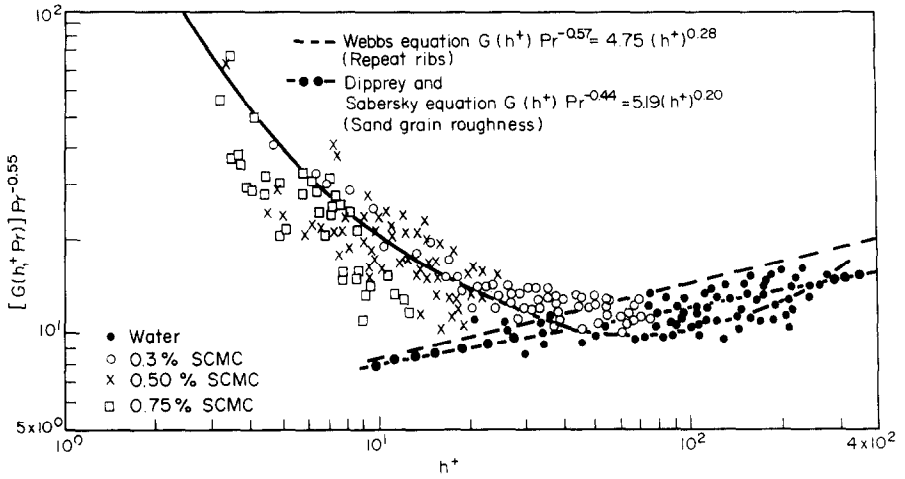

FIG. 7. Variation of $[G(h^+, Pr)]Pr^{-0.55}$ with roughness Reynolds number (h^+) for the heating of water and aqueous SCMC solutions in spirally corrugated tubes—final correlation.

Fig. 7. It is evident that spirally corrugated tubes do not exhibit fully rough friction factor behaviour, because they have only a low-to-medium-micro-roughness, and the dependence of G-function on (h^+) is less significant in the rough region $(h^+ > 25)$ compared to other rough surfaces.

Performance evaluation

In technically evaluating a spirally corrugated tube for a heat exchanger, a criterion of importance is the gain in internal heat transfer performance at constant pumping power, with the normal standard of comparison being a smooth tube of equal inside diameter. This criterion, referred to as R_3 by Bergles, Blumenkrantz and Taborek [23] ($R_3 = h_a/h_0$), is useful when the design objective is to increase the heat transfer capacity of an existing exchanger at constant pumping power to upgrade a process. For this criterion, we get

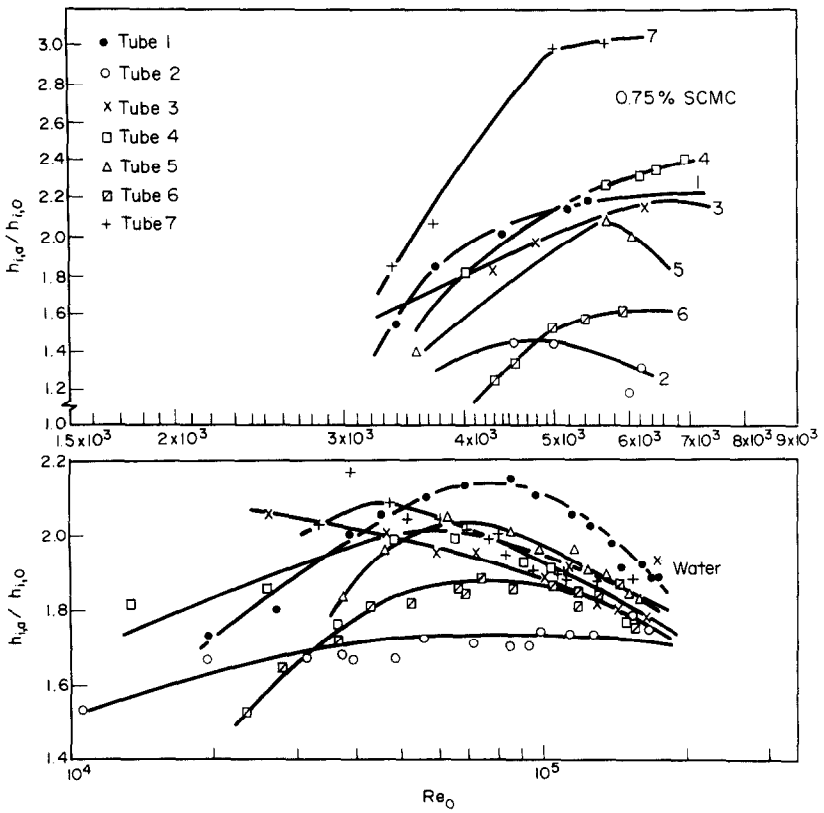

FIG. 8. Thermal performance of spirally corrugated tubes compared with a smooth tube at equal pumping power for the heating of water and 0.75% SCMC solution.

$$A_a f_a Re_a^3 = A_0 f_0 Re_0^3 = A_0(0.079)(Re_0)^{-0.25}(Re_0)^3$$

$$\therefore Re_0 = [12.66(A_a/A_0) f_a Re_a^3]^{0.364}$$

$$= 12.66 f_a (Re_a)^{0.364} \quad (22)$$

For the non-Newtonian polymer solutions, the Dodge–Metzner equation was used to obtain Re_0 as a function of f_0 for smooth tube. As this involved tedious and time-consuming calculations, empirical equations of the type $f_a = C_{(n)}[Re_0]^{m(n)}$, were obtained for each polymer solution. Obviously C and m are dependent on the flow behaviour index, n' of the test solution. The h_0 value was obtained corresponding to the calculated value of equivalent smooth tube Reynolds number, Re_0, using Dittus–Boelter equation for water and modified Dittus–Boelter equation for power law fluids.

The performance curves, showing $R_3(=h_a/h_0)$ vs Re_0 are shown in Fig. 8 for water and 0.75% SCMC for all the seven corrugated tubes used. For heating of water, all the tubes show a better thermal performance over the range $5 \times 10^4 < Re < 9 \times 10^4$. Of all the tubes, tube 1 has exhibited a performance ratio as high as 2.1. In general, the performance ratio for aqueous polymer solutions is higher than for water, and R values as high as 2.5–3 were obtained with the tube 7 with four helical starts, especially for 0.75% SCMC. In view of the more than two-fold increase in heat duty, multi-start spirally corrugated tubes appear to be attractive for convective heat transfer to fairly viscous fluids of high Prandtl number.

REFERENCES

1. J. Nikuradse, Law of flow in rough pipes, N.A.C.A. TM 1292 (1950).
2. D. F. Dipprey and R. H. Sabersky, Heat and momentum transfer in smooth and rough tubes at various Prandtl numbers, *Int. J. Heat Mass Transfer* **6**, 329–353 (1963).
3. R. A. Gowen and J. W. Smith, Turbulent heat transfer from smooth and rough surfaces, *Int. J. Heat Mass Transfer* **11**, 1657–1674 (1968).
4. N. Sheriff and P. Gumley, Heat transfer and friction properties of surfaces with discrete roughnesses, *Int. J. Heat Mass Transfer* **9**, 1297–1320 (1966).
5. R. L. Webb, E. R. G. Eckert and R. J. Goldstein, Heat transfer and friction in tubes with repeated rib roughness, *Int. J. Heat Mass Transfer* **14**, 601–617 (1971).
6. M. J. Lewis, Roughness functions—the thermohydraulic performance of rough surfaces and the Hall transformation—an overview, *Int. J. Heat Mass Transfer* **17**, 809–814 (1974).
7. M. Dalle Donne and E. Meyer, Turbulent convective heat transfer from surfaces with two-dimensional rectangular ribs, *Int. J. Heat Mass Transfer* **20**, 583–620 (1977).
8. D. L. Gee and R. L. Webb, Forced convection heat transfer in helically rib-roughened tubes, *Int. J. Heat Mass Transfer* **23**, 1127–1136 (1980).
9. A. P. Watkinson, D. L. Miletti and P. Tarassoff, Turbulent heat transfer and pressure drop in internally finned tubes, *A.I.Ch.E. Sym. Series*, **131**, 94–103 (1973).
10. T. C. Carnavos, Heat transfer performance of internally finned tubes in turbulent flow, *Symp. on Advances in Enhanced Heat Transfer*, pp. 61–67, *18th National Heat Transfer Conf.*, San Diego (1979).
11. P. Kumar and R. L. Judd, Heat transfer with coiled wire turbulence promotors, *Can. J. Chem. Eng.* **48**, 378–383 (1970).
12. J. W. Smith, R. A. Gowen and M. E. Charles, Turbulent heat transfer and temperature profiles in a riffled pipe, *Chem. Eng. Sci.* **23**, 751–758 (1968).
13. G. J. Kidd (Jr), Heat transfer and pressure drop characteristics of gas flow inside spirally corrugated tubes, *Am. Soc. Mech. Engs* Series C, *J. Heat Transfer* **92**, 513–519 (1970).
14. J. G. Withers, E. H. Young and W. B. Lampert, Heat transfer characteristics of corrugated tubes, *Chem. Engng Prog. Sym. Ser.* **174**, 15–24 (1978).
15. R. K. Gupta and M. Raja Rao, Heat transfer and friction characteristics of Newtonian and power law type of non-Newtonian fluids in smooth and spirally corrugated tubes, *Symp. on Enhanced Heat Transfer*, pp. 103–113, *18th National Heat Transfer Conf.*, San Diego (1979).
16. M. H. Mehta and M. Raja Rao, Heat transfer and frictional characteristics of spirally enhanced tubes for horizontal condensers, *Symp. on Enhanced heat transfer*, pp. 11–21, *18th National Heat Transfer Conf.*, San Diego (1979).
17. J. G. Withers, Tube-side heat transfer and pressure drop for tubes having helical internal ridging with turbulent/transitional flow of single-phase fluid—Part I single-helix ridging, *Heat Transfer Engng* **2**, 48–58 (1980).
18. J. Nikuradse, Gestz maßigkeit der turbulenten storomung in glatten Rohren, *Forschungscheft*, **XX**, 356 (1932).
19. D. W. Dodge and A. B. Metzner, Turbulent flow of non-Newtonian systems, *A.I.Ch.E. Jl* **5**, 189–204 (1954).
20. S. Ganeshan, Thermodynamics of spirally corrugated tubes, Ph.D. Thesis, Indian Institute of Technology, Bombay (1980).
21. R. M. Clapp, *International Developments in Heat Transfer* Part III, pp. 652–661, D-159, D-211-215. ASME, New York (1961).
22. A. H. P. Skelland, *Non-Newtonian flow and heat transfer*, p. 212. John Wiley, New York (1967).
23. A. E. Bergles, A. R. Blumenkrantz and J. Taborek, Performance evaluation criteria for enhanced heat transfer surfaces, *Proc. 5th Int. Heat Transfer Conference*, Tokyo, Vol. II, paper FC 6.3 (1974).

ETUDE THERMOHYDRAULIQUE DES TUBES CORRUGUES EN SPIRALE POUR L'EAU ET POUR DES FLUIDES A LOI PUISSANCE INDEPENDANTE DU TEMPS

Résumé—On présente des résultats expérimentaux sur le frottement pariétal et sur le comportement thermique d'un tube lisse et de sept tubes corrugués en spirales à un seul ou jusqu'à quatre départs helicoïdaux, ayant le même angle d'hélice 65° pour un domaine large de rapports de forme (h/D_i), (p/h) et (p/D_i) caractérisant la rugosité de la surface. Basées sur l'analogie entre transfert de chaleur et de quantité de mouvement, des relations sur le frottement et le transfert thermique sont développées pour représenter les données expérimentales. A partir du critère de la capacité de l'échangeur de chaleur par unité de puissance de pompage, les tubes corrugués à quatre départs sont trouvés être 100% plus efficaces qu'un tube lisse pour le chauffage de l'eau ($Pr = 4{,}3$) et 150% plus efficaces pour le chauffage des liquides les plus visqueux à grand nombre de Prandtl ($Pr_d = 109$).

THERMOHYDRAULISCHE UNTERSUCHUNGEN VON EIN- UND MEHRGÄNGIGEN SPIRALGEWELLTEN ROHREN FÜR WASSER UND FLUIDE, DIE ZEITUNABHÄNGIGEN POTENZGESETZEN FOLGEN

Zusammenfassung—Es werden experimentelle Untersuchungsergebnisse mitgeteilt über das Widerstands- und Wärmeübergangsverhalten von einem glatten Rohr und sieben ein- bis viergängigen spiralgewellten Rohren mit gleicher Steigung von 65° für einen großen Bereich von geometrischen Verhältnissen (h/D_i), (p/h) und (p/D_i), die die Oberflächenrauhigkeit charakterisieren. Auf der Grundlage der Analogie von Wärme- und Impulsübertragung wurden Widerstands- und Wärmeübergangsbeziehungen entwickelt und den experimentellen Daten angepaßt. Nach dem Kriterium der auf die Pumpenleistung bezogenen übertragbaren Wärmeleistung sind die viergängigen gewellten Rohre 100% leistungsfähiger als ein glattes Rohr bei der Erwärmung von Wasser ($Pr = 4{,}3$) und 150% leistungsfähiger bei Erwärmung von zäheren Flüssigkeiten mit großer Prandtl-Zahl ($Pr_d = 109$).

ИССЛЕДОВАНИЕ ТЕРМОГИДРАВЛИКИ ТРУБ С ОДНИМ И НЕСКОЛЬКИМИ СПИРАЛЬНО ЗАКРУЧЕННЫМИ ЖЕЛОБАМИ ПРИ ТЕЧЕНИИ ВОДЫ И НЕСТАЦИОНАРНЫХ СТЕПЕННЫХ ЖИДКОСТЕЙ

Аннотация — Представлены результаты экспериментального исследования поверхностного трения и теплопереноса одной гладкой трубы и семи гофрированных труб, имеющих от одного до четырех спирально нарезанных желобов с тем же углом закрутки в 65° и различными отношениями сторон (h/D_i), (p/h) и (p/D_i), характеризующими шероховатость поверхности. Исходя из аналогии между переносом тепла и импульса, предложены соотношения, описывающие экспериментальные данные по трению и теплопереносу. На основе критерия, характеризующего теплообменную емкость на единицу расхода энергии, найдено, что трубы с четырьмя желобами на 100% более эффективны, чем гладкая труба при течении нагретой воды ($Pr = 4{,}3$), и на 150% — при течении более вязких нагретых жидкостей с большим числом Прандтля ($Pr_d = 109$).